Quasi-phase matching and characterization of high-order harmonic generation in hollow waveguides using counterpropagating light

Amy L. Lytle*, Xiaoshi Zhang, Richard L. Sandberg, Oren Cohen, Henry C. Kapteyn, and Margaret M. Murnane

JILA, University of Colorado, Boulder, CO 80309 USA
**Corresponding author: lytle@colorado.edu*

Abstract: We review recent experimental and theoretical work on the use of counterpropagating light to enhance high-order harmonic generation through all-optical quasi-phase matching. Also presented is a new technique for measuring the coherence of high harmonics in the nonlinear medium. This information is crucial for understanding the process of harmonic generation over extended distances, as well as for effective enhancement using quasi-phase matching techniques.

OCIS codes: (190.7110) Ultrafast nonlinear optics, (190.2620) Harmonic generation and ixing

References and links

1. H. C. Kapteyn, O. Cohen, I. Christov, and M. M. Murnane, "Harnessing Attosecond Science in the Quest for Coherent X-Rays," Science **317**, 775 (2007).
2. H. C. Kapteyn, M. M. Murnane, and I. P. Christov, "Extreme Nonlinear Optics: Coherent X-rays from Lasers," Phys. Today **58**, 5 (2005).
3. I. P. Christov, M. M. Murnane, and H. C. Kapteyn, "High-Harmonic Generation of Attosecond Pulses in the "Single-Cycle" Regime," Phys. Rev. Lett. **78**, 1251 - 1254 (1997).
4. R. Kienberger, E. Goulielmakis, M. Uiberacker, A. Baltuska, V. Yakovlev, F. Bammer, A. Scrinzi, T. Westerwalbesloh, U. Kleineberg, U. Heinzmann, M. Drescher, and F. Krausz, "Atomic transient recorder," Nature **427**, 817-821 (2004).
5. P. M. Paul, E. S. Toma, P. Breger, G. Mullot, F. Auge, P. Balcou, H. G. Muller, and P. Agostini, "Observation of a train of attosecond pulses from high harmonic generation," Science **292**, 3 (2001).
6. R. A. Bartels, A. Paul, H. Green, H. C. Kapteyn, M. M. Murnane, S. Backus, I. P. Christov, Y. Liu, D. T. Attwood, and C. Jacobsen, "Fully spatially coherent EUV beams generated using a small-scale laser," Science **297**, 376 - 378 (2002).
7. M. Bellini, C. Lynga, A. Tozzi, M. B. Gaarde, T. W. Hansch, A. L'Huillier, and C. G. Wahlstrom, "Temporal coherence of ultrashort high-order harmonic pulses," Phys. Rev. Lett. **81**, 297-300 (1998).
8. R. Sandberg, A. Paul, D. Raymondson, S. Hädrich, D. Gaudiosi, J. Holtsnider, R. Tobey, O. Cohen, M. Murnane, H. Kapteyn, C. Song, J. Miao, Y. Liu, and F. Salmassi, "Lensless diffractive imaging using coherent high harmonic beams," Phys. Rev. Lett. **99**, 098103 (2007).
9. R. I. Tobey, M. E. Siemens, O. Cohen, M. M. Murnane, and H. C. Kapteyn, "Ultrafast Extreme Ultraviolet Holography: Dynamic Monitoring of Surface Deformation," Opt. Lett. **32**, 286 (2007).
10. M. Wieland, C. Spielmann, U. Kleineberg, T. Westerwalbesloh, U. Heinzmann, and T. Wilhein, "Toward time-resolved soft X-ray microscopy using pulsed fs-high-harmonic radiation," Ultramicroscopy **102**, 93-100 (2005).
11. A. Baltuska, T. Udem, M. Uiberacker, M. Hentschel, E. Goulielmakis, C. Gohle, R. Holzwarth, V. S. Yakoviev, A. Scrinzi, T. W. Hansch, and F. Krausz, "Attosecond control of electronic processes by intense light fields," Nature **421**, 611-615 (2003).
12. T. Kanai, S. Minemoto, and H. Sakai, "Quantum interference during high-order harmonic generation from aligned molecules," Nature **435**, 470-474 (2005).
13. X. B. Zhou, R. Lock, W. Li, N. Wagner, M. M. Murnane, and H. C. Kapteyn, "Molecular recollision interferometry in high harmonic generation," Phys. Rev. Lett. **100**, 073902 (2008).
14. N. Wagner, A. Wüest, I. Christov, T. Popmintchev, X. Zhou, M. Murnane, and H. Kapteyn, "Monitoring Molecular Dynamics using Coherent Electrons from High-Harmonic Generation," Proc. Nat. Acad. Sci USA **103**, 13279 (2006).
15. E. Gagnon, P. Ranitovic, C. L. Cocke, M. M. Murnane, H. C. Kapteyn, and A. S. Sandhu, "Soft X-ray driven femtosecond molecular dynamics," Science **317**, 1374 (2007).
16. H. Niikura, F. Legare, R. Hasbani, M. Y. Ivanov, D. M. Villeneuve, and P. B. Corkum, "Probing molecular dynamics with attosecond resolution using correlated wave packet pairs," Nature **421**, 826-829 (2003).

#92162 - $15.00 USD Received 28 Jan 2008; revised 15 Apr 2008; accepted 19 Apr 2008; published 24 Apr 2008

17. J. Itatani, J. Levesque, D. Zeidler, H. Niikura, H. Pepin, J. C. Kieffer, P. B. Corkum, and D. M. Villeneuve, "Tomographic imaging of molecular orbitals," Nature **432**, 867–871 (2004).
18. L. Miaja, G. Saathoff, T. Lei, M. Murnane, H. Kapteyn, M. Aeschlimann, and J. Gland, "Observation of the Laser-Assisted Photoelectric Effect on Pt(111)," Phys. Rev. Lett. **97**, 113604 (2006).
19. M. Drescher, M. Hentschel, R. Kienberger, M. Uiberacker, V. Yakovlev, A. Scrinizi, T. Westerwalbesloh, U. Kleineberg, U. Heinzmann, and F. Krausz, "Time-resolved atomic inner-shell spectroscopy," Nature **419**, 803-807 (2002).
20. P. B. Corkum, "Plasma perspective on strong-field multiphoton ionization," Phys. Rev. Lett. **71**, 4 (1993).
21. M. Lewenstein, P. Balcou, M. Y. Ivanov, A. L'Huillier, and P. B. Corkum, "Theory of high-harmonic generation by low-frequency laser fields," Phys. Rev. A **49**, 15 (1994).
22. K. C. Kulander, K. J. Schafer, and J. L. Krause, "Dynamics of short-pulse excitation, ionization, and harmonic conversion," in *Super-Intense Laser-Atom Physics*, A. L. H. B. Piraux, and K. Rzazewski, ed., (Plenum, Han-sur-Lesse, Belgium, 1993), pp. 95-110.
23. E. Seres, J. Seres, and C. Spielmann, "X-ray absorption spectroscopy in the keV range with laser generated high harmonic radiation," App. Phys. Lett. **89**, 181919 (2006).
24. P. Salieres, A. L'Huillier, and M. Lewenstein, "Coherence Control of High-Order Harmonics," Phys. Rev. Lett. **74**, 3776-3779 (1995).
25. A. Rundquist, C. G. Durfee, Z. H. Chang, C. Herne, S. Backus, M. M. Murnane, and H. C. Kapteyn, "Phase-matched generation of coherent soft x-rays," Science **280**, 1412-1414 (1998).
26. X. Zhang, A. R. Libertun, A. Paul, E. Gagnon, S. Backus, I. P. Christov, M. M. Murnane, H. C. Kapteyn, R. A. Bartels, Y. Liu, and D. T. Attwood, "Highly coherent light at 13 nm generated by use of quasi-phase-matched high-harmonic generation," Opt. Lett. **29**, 1357-1359 (2004).
27. A. L. Lytle, X. Zhang, P. Arpin, O. Cohen, M. M. Murnane, and H. C. Kapteyn, "Quasi-phase matching of high order harmonic generation at high photon energies using counterpropagating pulses," Opt. Lett. **33**,174-176 (2008).
28. J. Zhou, J. Peatross, M. M. Murnane, and H. C. Kapteyn, "Enhanced high-harmonic generation using 25 fs laser pulses," Phys. Rev. Lett. **76**, 752-755 (1996).
29. T. Brabec, and F. Krausz, "Intense few-cycle laser fields: Frontiers of nonlinear optics," Rev. Mod. Phys. **72**, 545-591 (2000).
30. E. A. Gibson, A. Paul, N. Wagner, R. Tobey, S. Backus, I. P. Christov, M. M. Murnane, and H. C. Kapteyn, "High-order harmonic generation up to 250 eV from highly ionized argon," Phys. Rev. Lett. **92**, 4 (2004).
31. D. M. Gaudiosi, B. Reagan, T. Popmintchev, M. Grisham, M. Berrill, O. Cohen, B. C. Walker, M. M. Murnane, H. C. Kapteyn, and J. J. Rocca, "High-order harmonic generation from ions in a capillary discharge," Phys. Rev. Lett. **96**, 203001 (2006).
32. P. Colosimo, G. Doumy, C. I. Blaga, J. Wheeler, C. Hauri, F. Catoire, J. Tate, R. Chirla, A. M. March, G. G. Paulus, H. G. Muller, P. Agostini, and L. F. DeMauro, "Scaling strong-field interactions towards the classical limit," Nature Phys. Advance Online Publication 23 March 2008 (doi:10.1038/nphys914)
33. A. Gordon, and F. X. Kartner, "Scaling of keV HHG photon yield with drive wavelength," Opt. Express **13**, 2941-2947 (2005).
34. B. Shan, and Z. H. Chang, "Dramatic extension of the high-order harmonic cutoff by using a long-wavelength driving field," Phys. Rev. A **65**, 011804 (2002).
35. T. O. Clatterbuck, C. Lynga, P. Colosimo, J. D. D. Martin, B. Sheehy, L. F. Dimauro, P. Agostini, and K. C. Kulander, "Scaled intense laser-atom physics: the long wavelength regime," J. Mod. Opt. **50**, 441-450 (2003).
36. J. Tate, T. Auguste, H. G. Muller, P. Salieres, P. Agostini, and L. F. DiMauro, "Scaling of wave-packet dynamics in an intense midinfrared field," Phys. Rev. Lett. **98**, 013901 (2007).
37. V. S. Yakovlev, M. Ivanov, and F. Krausz, "Enhanced phase-matching for generation of soft X-ray harmonics and attosecond pulses in atomic gases," Opt. Express **15**, 15351-15364 (2007).
38. T. Popmintchev, M.-C. Chan, O. Cohen, M. Grisham, J. J. Rocca, M. M. Murnane, and H. C. Kapteyn, "Extended Phase-Matching of High-Order Harmonics Driven by Mid-Infrared Light," Opt. Lett. (submitted for publication).
39. J. A. Armstrong, N. Bloembergen, J. Ducuing, and P. S. Pershan, "Interactions between Light Waves in a Nonlinear Dielectric," Phys. Rev. **127**, 1918 (1962).
40. M. M. Fejer, "Nonlinear-Optical Frequency-Conversion," Phys. Today **47**, 25-32 (1994).
41. M. M. Fejer, G. A. Magel, D. H. Jundt, and R. L. Byer, "Quasi-Phase-Matched 2nd Harmonic-Generation - Tuning and Tolerances," IEEE J. Quantum Electron. **28**, 2631-2654 (1992).
42. R. L. Byer, "Quasi-phasematched nonlinear interactions and devices," J. Nonlinear Opt. Phys. & Mat. **6**, 549-592 (1997).
43. I. P. Christov, M. M. Murnane, and H. C. Kapteyn, "Quasi-phase matching of high-harmonics and attosecond pulses in modulated waveguides," Opt. Express **7**, 5 (2000).
44. B. Dromey, M. Zepf, M. Landreman, and S. M. Hooker, "Quasi-phasematching of harmonic generation via multimode beating in waveguides," Opt. Express **15**, 7894-7900 (2007).
45. J. Peatross, M. V. Fedorov, and K. C. Kulander, "Intensity-Dependent Phase-Matching Effects in Harmonic-Generation," J. Opt. Soc. Am. B **12**, 7 (1995).
46. J. Peatross, S. Voronov, and I. Prokopovich, "Selective zoning of high harmonic emission using counter-propagating light," Opt. Express **1**, 114-124 (1997).

#92162 - $15.00 USD Received 28 Jan 2008; revised 15 Apr 2008; accepted 19 Apr 2008; published 24 Apr 2008

47. O. Cohen, T. Popmintchev, D. M. Gaudiosi, M. M. Murnane, and H. C. Kapteyn, "Unified microscopic-macroscopic formulation of high-order difference-frequency mixing in plasmas," Phys. Rev. Lett. **98**, 043903 (2007).
48. O. Cohen, X. Zhang, A. L. Lytle, T. Popmintchev, M. M. Murnane, and H. C. Kapteyn, "Grating-Assisted Phase Matching in Extreme Nonlinear Optics," Phys. Rev. Lett. **99**, 053902 (2007).
49. T. Pfeifer, and M. C. Downer, "Direct experimental observation of periodic intensity modulation along a straight hollow-core optical waveguide," J. Opt. Soc. Am. B **24**, 1025-1029 (2007).
50. P. L. Shkolnikov, A. Lago, and A. E. Kaplan, "Optimal quasi-phase-matching for high-order harmonic-generation in gases and plasma," Phys. Rev. A **50**, R4461-R4464 (1994).
51. T. Auguste, B. Carre, and P. Salieres, "Quasi-phase-matching of high-order harmonics using a modulated atomic density," Phys. Rev. A **76**, 011802 (2007).
52. J. Seres, V. Yakovlev, E. Seres, C. Streli, P. Wobrauschek, C. Spielmann, and F. Krausz, "Coherent superposition of laser-driven soft-X-ray harmonics from successive sources," Nat. Phys. **3**, 878-883 (2007).
53. A. Paul, R. A. Bartels, R. Tobey, H. Green, S. Weiman, I. P. Christov, H. C. Kapteyn, M. M. Murnane, and S. Backus, "Quasi phase matched generation of coherent extreme ultraviolet light," Nature **421**, 51 (2003).
54. E. A. Gibson, A. Paul, N. Wagner, R. Tobey, D. Gaudiosi, S. Backus, I. P. Christov, A. Aquila, E. M. Gullikson, D. T. Attwood, M. M. Murnane, and H. C. Kapteyn, "Coherent soft x-ray generation in the water window with quasi-phase matching," Science **302**, 95-97 (2003).
55. X. S. Zhang, A. Lytle, T. Popmintchev, A. Paul, N. Wagner, M. Murnane, H. Kapteyn, and I. P. Christov, "Phase matching, quasi-phase matching, and pulse compression in a single waveguide for enhanced high-harmonic generation," Opt. Lett. **30**, 3-5 (2005).
56. M. Zepf, B. Dromey, M. Landreman, P. Foster, and S. M. Hooker, "Bright Quasi-Phase-Matched Soft-X-Ray Harmonic Radiation from Argon Ions," Phys. Rev. Lett. **99**, 143901 (2007).
57. A. L. Lytle, X. Zhang, J. Peatross, M. M. Murnane, H. C. Kapteyn, and O. Cohen, "Probe of high-order harmonic generation using counterpropagating light in a hollow waveguide," Phys. Rev. Lett. **98**, 123904 (2007).
58. X. Zhang, A. L. Lytle, T. Popmintchev, X. Zhou, M. M. Murnane, H. C. Kapteyn, and O. Cohen, "Quasi-phase matching and quantum path control of high harmonic generation using counterpropagating light," Nature Phys. **3**, 270-275 (2007).
59. O. Cohen, A. L. Lytle, X. Zhang, M. M. Murnane, and H. C. Kapteyn, "Optimizing quasi-phase matching of high harmonic generation using counter propagating pulse trains," Opt. Lett. **32**, 2975-2977 (2007).
60. X. Zhang, A. L. Lytle, O. Cohen, M. M. Murnane, and H. C. Kapteyn, "Quantum path control in high-order harmonic generation at high photon energies," New J. Phys. **10**, 025021 (2008).
61. M. Landreman, K. O'Keefe, T. Robinson, M. Zepf, B. Dromey, and S. Hooker, "Comparison of parallel and perpendicular polarized counterpropagating light for suppressing high harmonic generation," J. Opt. Soc. Am. B **24**, 2421-2427 (2007).
62. R. Bartels, S. Backus, I. Christov, H. Kapteyn, and M. Murnane, "Attosecond time-scale feedback control of coherent X-ray generation," Chem. Phys. **267**, 277-289 (2001).
63. R. Bartels, S. Backus, E. Zeek, L. Misoguti, G. Vdovin, I. P. Christov, M. M. Murnane, and H. C. Kapteyn, "Shaped-pulse optimization of coherent soft-x-rays," Nature **406**, 164-166 (2000).
64. I. P. Christov, R. Bartels, H. C. Kapteyn, and M. M. Murnane, "Attosecond time-scale intra-atomic phase matching of high harmonic generation," Phys. Rev. Lett. **86**, 5458-5461 (2001).
65. M. Lewenstein, P. Salieres, and A. L'Huillier, "Phase of the atomic polarization in high-order harmonic generation," Phys. Rev. A **52**, 4747 (1995).
66. Z. Chang, A. Rundquist, H. Wang, I. Christov, H. C. Kapteyn, and M. M. Murnane, "Temporal phase control of soft-x-ray harmonic emission," Phys. Rev. A **58**, R30-R33 (1998).
67. N. Wagner, E. Gibson, T. Popmintchev, I. Christov, M. Murnane, and H. Kapteyn, "Self-compression of ultrashort pulses through ionization-induced spatio-temporal reshaping," Phys. Rev. Lett. **93**, 173902 (2004).
68. P. D. Maker, R. W. Terhune, M. Nisenoff, and C. M. Savage, "Effects of dispersion and focusing on the production of optical harmonics," Phys. Rev. Lett. **8**, 4 (1962).
69. S. Kazamias, D. Douillet, C. Valentin, F. Weihe, F. Auge, T. Lefrou, G. Grillon, S. Sebban, and P. Balcou, "Observation of high-contrast coherence fringes in high-order harmonic generation," Phys. Rev. A **68**, 7 (2003).
70. E. Constant, D. Garzella, P. Breger, E. Mevel, C. Dorrer, C. Le Blanc, F. Salin, and P. Agostini, "Optimizing high harmonic generation in absorbing gases: Model and experiment," Phys. Rev. Lett. **82**, 4 (1999).
71. M. V. Ammosov, N. B. Delone, and V. P. Krainov, "Tunnel ionization of complex atoms and atomic ions in a varying electromagnetic field," Zh. Eksp. Teor. Fiz. (Sov. Phys. JETP) **91**, 2008-2012 (1986).
72. C. P. Hauri, W. Kornelis, F. W. Helbing, A. Heinrich, A. Couairon, A. Mysyrowicz, J. Biegert, and U. Keller, "Generation of intense, carrier-envelope phase-locked few-cycle pulses through filamentation," Appl. Phys. B **79**, 673-677 (2004).
73. E. A. J. Marcatili, and R. A. Schmeltzer, "Hollow Metallic and Dielectric Waveguides for Long Distance Optical Transmission and Lasers," Bell Syst. Tech. J. **43**, 24 (1964).
74. S. L. Voronov, I. Kohl, J. B. Madsen, J. Simmons, N. Terry, J. Titensor, Q. Wang, and J. Peatross, "Control of Laser High-Harmonic Generation with Counterpropagating Light," Phys. Rev. Lett. **87**, 133902 (2001).
75. J. R. Sutherland, E. L. Christensen, N. D. Powers, S. E. Rhynard, J. C. Painter, and J. Peatross, "High harmonic generation in a semi-infinite gas cell," Opt. Express **12**, 6 (2004).
76. Z. Chang, A. Rundquist, H. Wang, I. Christov, H. C. Kapteyn, and M. M. Murnane, "Temporal phase control of soft-x-ray harmonic emission," Phys. Rev. A **58**, R30-R33 (1998).

#92162 - $15.00 USD Received 28 Jan 2008; revised 15 Apr 2008; accepted 19 Apr 2008; published 24 Apr 2008

77. H. J. Shin, D. G. Lee, Y. H. Cha, J.-H. Kim, K. H. Hong, and C. H. Nam, "Nonadiabatic blueshift of high-order harmonics from Ar and Ne atoms in an intense femtosecond laser field," Phys. Rev. A **63**, 053407 (2001).
78. B. A. Reagan, T. Popmintchev, M. E. Grisham, D. M. Gaudiosi, M. Berrill, O. Cohen, B. C. Walker, M. M. Murnane, J. J. Rocca, and H. C. Kapteyn, "Enhanced high-order harmonic generation from Xe, Kr, and Ar in a capillary discharge," Phys. Rev. A **76**, 013816 (2007).

1. Introduction

The process of high-order harmonic generation (HHG) has been studied extensively as a source of coherent extreme ultraviolet (EUV) and soft x-ray light with ultrashort (fs-to-as) pulse duration [1-5]. The high temporal and spatial coherence [6, 7] of HHG-based light sources makes possible applications such as coherent imaging [8-10] and studies of atomic, molecular and surface dynamics [11-19]. Moreover, since high harmonics can be generated by a desktop, few-millijoule, femtosecond laser system, this source is both accessible and versatile.

The extreme nonlinear optics of HHG involves a coherent electron rescattering. First, an intense, ultrashort laser pulse field-ionizes an atom. The free electron moves under the influence of the laser field, and can recollide with the parent ion within a fraction of an optical cycle, emitting a high-energy photon [20, 21]. The photon energy obtained using the HHG process scales linearly with the applied laser intensity according to the cutoff rule, which is given by –

$$h\upsilon_{\max} = I_p + 3.2U_p, \tag{1}$$

where I_p is the ionization potential of the gas and the ponderomotive potential $U_p \propto I\lambda^2$, where I and λ are the intensity and wavelength of the driving laser, is the quiver energy of the liberated electron [22]. This very favorable cutoff rule, which is linear in applied laser intensity, allows very high harmonics to be generated, up to photon energies exceeding 1 keV [23]. However, most experimental applications of HHG-based light sources to date have made use of coherent light with photon energy $h\nu <\approx 100$ eV, because phase matched frequency conversion is possible only for low photon energies. In a phase-matched nonlinear optical process, the high-order nonlinear polarization excited by the driving laser pulse and the generated high-order harmonic light travel with the same phase velocity through the medium. Under this condition, high-order harmonic light generated throughout the nonlinear medium adds constructively, leading to a bright and coherent high harmonic beam at the exit of the medium. On the other hand, if the conversion process is not phase matched, the high harmonic signal builds up only over a propagation distance where the relative phase of the driving laser and harmonic fields slip by π radians. This distance is the coherence length $L_c = \pi/\Delta k$, where Δk is the phase mismatch between the driving laser and harmonic fields.

One very effective approach for obtaining true phase matched high harmonic generation involves creating a near plane-wave propagation geometry by propagating high-intensity light inside a hollow waveguide. In this geometry, the major sources of phase mismatch are due to both pressure-dependent (neutral and free electron plasma dispersion) and pressure-independent (geometrical from free-focusing [24] or waveguide [25] propagation) terms. In this case, the conversion efficiency can be optimized by varying the gas pressure inside the waveguide, to eliminate the phase mismatch –

$$\Delta k = q\left\{\left(\frac{u_{11}^2\lambda_0}{4\pi a^2}\right) - P\left((1-\eta)\frac{2\pi}{\lambda_0}\delta n - \eta\left[N_{atm}r_e\lambda_0\right]\right)\right\}, \tag{2}$$

In Eq. (2), q is the harmonic order, u_{11} is the lowest-order waveguide mode factor, λ_o is the center wavelength of the driving laser, a is the inner radius of the hollow waveguide, P is the pressure, η is the ionization level, r_e is the classical electron radius, N_{atm} is the number density of atoms at 1 atm, and δn is the difference between the indices of refraction of helium at the

#92162 - $15.00 USD Received 28 Jan 2008; revised 15 Apr 2008; accepted 19 Apr 2008; published 24 Apr 2008

fundamental and harmonic wavelengths. The result is a light source with both a useful conversion efficiency of laser light to short wavelengths (~10^{-5} to photon energies ~45 eV using argon gas as a nonlinear medium), and with diffraction-limited coherent beam characteristics [6, 26].

However, for photon energies >50 eV using argon gas, and >~110 eV using helium gas, phase matching of the high harmonic conversion process is no longer possible. This is because the higher required incident laser intensity needed to generate these harmonics results in a much higher level of ionization in the medium. The resulting free-electron dispersion leads to an uncompensatable phase mismatch for ionization levels higher than a critical ionization fraction η_{cr} [27], which from Eq. (2) is given by –

$$\eta_{cr} = \left[\left(\frac{\lambda_o N_{atm}}{2\pi\delta n} \right) \left(1 - \frac{1}{q^2} \right) + 1 \right]^{-1}. \tag{3}$$

Above this critical ionization level (≈ 5% for argon and ≈ 0.5% for helium using a 0.8 μm wavelength driving laser), the phase mismatch due to the plasma cannot be eliminated by adjusting the gas pressure or focusing geometry. At higher levels of ionization, the uncompensated plasma dispersion can reduce L_c to tens of microns. The use of very short ~<25 fs driving laser pulses is very useful for optimizing conversion efficiency since it allows for a high incident intensity with minimum pulse energy and level of ionization of the gas [28]. However, the comparative advantage of shorter and shorter pulses in terms of conversion efficiency diminishes for pulses substantially shorter than 20 fs due to nonadiabatic effects [3, 29].

Use of a longer wavelength driving laser or higher laser intensity can significantly extend the cutoff photon energy from both atoms and ions [30, 31]. For example, the favorable λ^2 scaling has motivated studies of HHG with mid-infrared driving pulses [32, 33]. Significant extension of the cutoff energy was demonstrated in several experiments [32, 34, 35]. However, it was recently found both theoretically and experimentally that the single-atom yield scales as $\lambda^{-5.5\pm0.5}$, which greatly reduces the efficiency of HHG driven by longer wavelengths [36]. Thus, increasing the HHG yield by phase-matching the conversion process is critical to obtain a usable flux even using infrared driving lasers. Indeed, it was recently suggested theoretically that favorable "self phase matching" conditions might be realized with mid-IR pulses [37]. Other recent experimental and theoretical work has shown that it is possible to extend true phase-matching of the high harmonic generation process to significantly higher photon energies (in theory to ~1 keV) using long wavelength driving lasers [38]. However, the unfavorable single atom yield may limit applications of harmonics driven by long wavelength drivers to photon energies ~300 eV, even when perfectly phase matched.

Thus, for efficient high harmonic generation at high photon energies, new approaches are needed to compensate for phase mismatch. In conventional low-order nonlinear optics (i.e., second harmonic generation, etc), quasi-phase matching (QPM) is widely employed as an alternative to true phase matching [39-41]. Instead of creating a geometry where the phase velocities of the driving laser and harmonic beams match throughout the entire interaction region, in QPM the phase mismatch is periodically corrected. This correction thus prevents back-conversion of the generated harmonic light. Many QPM techniques used in the visible region of the spectrum involve design of the appropriate periodic variations in the crystalline structure of the nonlinear material [42]. For HHG, where the nonlinear medium is a low-density plasma, proposals for QPM have involved a periodic variation in either the intensity of the laser field [43-49] or the density of the gas [50-52].

Three techniques for quasi phase matching of the HHG process have been demonstrated experimentally to date. In the first approach, the driving laser intensity is varied by modulating the inner diameter of a hollow waveguide, while the gas pressure and laser intensity are tuned to match the coherence length to the waveguide and laser modulation period [53, 54]. QPM using a modulated waveguide structure, however, only partially

#92162 - $15.00 USD Received 28 Jan 2008; revised 15 Apr 2008; accepted 19 Apr 2008; published 24 Apr 2008

compensates for the phase mismatch. This is because propagation effects in the waveguide, such as mode beating, ionization and guiding loss, refraction, and group velocity dispersion lead to a dynamically changing laser intensity in both space and time along the propagation direction of the driving laser. These changes in-turn result in a longitudinally-varying phase mismatch (coherence length) which is difficult to compensate for over more than a few coherence lengths using a rigidly modulated waveguide. As a result, significant enhancements of 1-2 orders of magnitude were demonstrated. Related work that investigated high harmonic generation waveguides under highly ionized conditions used plasma-induced spatio-temporal coupling and modebeating to vary the laser intensity, instead of a modulated waveguide [55, 56]. However, all these improvements are much less than is in-principle possible under full phase matching conditions that coherently combine the emission over extended distances and many coherence lengths. More recently, Seres, *et al*., [52] demonstrated a QPM technique by periodic modulation of the gas pressure in a free-space focus geometry. Enhancement factors of $\approx$ 4 were achieved at very short wavelengths of ~2-5 nm by optimizing the distance between two regions of high gas density along the axis of laser propagation. However, the scalability to higher enhancements appears to be limited in this geometry.

In recent work [27, 57-60], we demonstrated experimentally that the use of counterpropagating pulse trains is a flexible and practical alternative for implementing all-optical quasi phase matching of the high harmonic upconversion process in hollow waveguides. This approach to extreme QPM is based on the fact that wherever a relatively weak counterpropagating pulse intersects with the driving laser pulse, the coherent buildup of the harmonic field is suppressed [46, 59, 61]. Thus QPM can be achieved by suppressing harmonic emission from destructively interfering, out-of-phase regions in the medium, permitting buildup of the harmonic signal over a longer interaction length [27, 58]. Furthermore, the counterpropagating light pattern can be manipulated to compensate for a dynamically changing phase mismatch, a crucial improvement over all previous techniques. Counterpropagating pulses have also been demonstrated as a tool for probing the local coherent buildup in a hollow waveguide geometry [57], providing crucial information for effective implementation of all-optical QPM. Further progress depends on understanding what factors influence coherent buildup in a non-uniform plasma medium and on implementing more sophisticated techniques for generating counterpropagating pulse trains and infrared fields [48] with adjustable duration, separation, and intensity.

This paper is organized as follows. In Section 2, we review theoretical work that investigated the influence of a counterpropagating light pulse on HHG as well as the use of counterpropagating train of pulses for QPM of the HHG process. In Section 3, we discuss recent work that used a single counterpropagating pulse to measure the in-situ coherence length of HHG in waveguides. Section 4 presents new information that can be extracted by probing the coherence properties of HHG in waveguides using two counterpropagating pulses. In Section 5, we summarize recently published work demonstrating significant enhancement of HHG around 70 eV and 140 eV, using all-optical QPM with counterpropagating pulse trains. Section 6 describes how this work can lead to a better understanding of propagation effects on HHG, and how this information can be exploited to implement new and improved phase matching schemes at higher, keV, photon energies.

2. Counterpropagating light in HHG: theoretical studies

Because high harmonic generation involves a coherent electron rescattering process, the time interval between ionization and rescattering means that the phase of the rescattering electron (and hence the phase of the high-order polarization and emitted HHG field) is not rigidly related to the phase of the driving laser field. The quantum phase of the electron evolves between ionization and rescattering and is proportional to the applied laser intensity. Thus intensity or phase modulations either in the driving laser field, or induced by a second laser field, can be used to manipulate the phase of the rescattering electron on an attosecond time scale, and as a result, the phase of the harmonic emission [62-64].

#92162 - $15.00 USD Received 28 Jan 2008; revised 15 Apr 2008; accepted 19 Apr 2008; published 24 Apr 2008

The effects of counterpropagating light on the HHG process was theoretically investigated first by Peatross, *et al.*, [46], and more recently by Cohen, *et al.*, [59] and Landreman, *et al.* [61]. In the region where the driving laser pulse and a relatively long and weak counterpropagating pulse overlap, a standing modulation in both the laser intensity and phase is formed, with periodicity of half the laser wavelength ($\Lambda = \lambda_o/2$) (see Fig. 1). These rapid modulations can microscopically disrupt coherent buildup of harmonic emission, either directly through the phase modulation, or through the intensity-dependent phase, essentially by scrambling the harmonic phase in any region where the two laser beams intersect.

Coherent harmonic buildup can be suppressed by a relatively weak counterpropagating field strength. It can be shown [61] that the magnitude of the phase modulation of the fundamental laser field, $\Delta\Phi_P$, is approximately equal to $2E_C/E_F$, or twice the ratio of the counter to the forward propagating field. Thus, the laser phase modulation $\Delta\Phi_P$ and the counterpropagating field E_c can be quite small ($\sim 10^{-3}$) while the magnitude of the phase modulation on the generated harmonic is a factor of q larger, where q is the harmonic order. When the magnitude of the phase oscillation is equal to π radians, emission from sections that are separated by $\Lambda/2$ have opposite phases and therefore interfere destructively. In other words, the effective coherence length in the region where the counterpropagating beams intersect is now $L_c = \Lambda/2$, or << 1 μm. Thus, harmonic field buildup is effectively suppressed in the overlap region between the two pulses. Moreover, because the induced phase modulation of the harmonic field is proportional to the harmonic order q, the higher the harmonic order, the less intense the counterpropagating beam needed for efficient suppression. Detailed numerical calculations have shown that even weak counterpropagating pulses (intensity ratio of 10^{-2} – 10^{-6}, depending on the harmonic order) are sufficient to significantly suppress harmonic emission. This fact is critical to practical implementation of QPM using counterpropagating light. Although the pulse driving the harmonic generation process can be very short, a counterpropagating pulse sequence ideally needs to intersect with the driving pulse over a length comparable to the *entire medium*. Thus, the required pulse train will typically have duration in the >>1 ps range.

The intrinsic intensity-dependent phase shift $\Delta\Phi_I$, acquired by the electron during its trajectory in the continuum is linear in the laser intensity and can reach tens to hundreds of radians [65, 66]. Consequently, the slight and rapid sinusoidal modulation in the intensity of the harmonic generating field, $\Delta I(z)$ can also cause a significant phase modulation:

$$\Delta\Phi_I(z) \propto \Delta I(z) \propto E_F^2 r \cos(2\pi z/\Lambda). \tag{4}$$

In Eq. (4), E_F is the amplitude of the driving laser field, r is the ratio of the amplitudes of the counter- to the forward-propagating fields, z is the propagation distance, and $\Lambda = \lambda_o/2$ is the period of the laser intensity modulation.

As an example of how the harmonic field may be suppressed by phase modulations, we consider the microscopic effective emission factor in the presence of an intensity-dependent phase modulation [59]. The microscopic effective emission factor is the ratio between the generated harmonic field with and without the presence of counterpropagating light, over one period of the standing wave. It is given by –

$$\xi = \frac{1}{\Lambda}\int_0^{\Lambda} \exp[i\Delta\Phi_I(z)]dz = \frac{1}{\Lambda}\int_0^{\Lambda} \exp\left[iA\cos\left(\frac{2\pi}{\Lambda}z\right)\right]dz = J_0(A). \tag{5}$$

In Eq. (2), J_o is the zero-order Bessel function of the first kind and A is the amplitude of the induced phase modulation. Clearly, the presence of the counterpropagating field suppresses the harmonic emission, since $|\xi(A \neq 0)| < 1$. Moreover, the microscopic effective emission factor can be zero or even negative. This latter case corresponds to an extra π phase shift for HHG.

Harmonic emission in the presence of a counterpropagating field with a polarization perpendicular to that of the driving laser has also been investigated [61]. In this case, the

#92162 - $15.00 USD Received 28 Jan 2008; revised 15 Apr 2008; accepted 19 Apr 2008; published 24 Apr 2008

combined fields of the forward and counterpropagating pulses in the intersection region have an elliptic polarization, which suppresses the HHG process by reducing the probability that the ionized electron will recombine with its parent ion. It was found that, for efficient suppression of HHG, this scheme required counterpropagating pulses with much larger intensities than in the case of parallel polarization.

To implement true QPM, a train of counterpropagating pulses is needed to suppress harmonic generation in several selected out-of-phase regions of the medium. As illustrated in Fig. 1, when the phase mismatch is nonzero, the harmonic signal oscillates with a period of twice the coherence length. The harmonic field increases until the phase slip between the driving laser and harmonic fields reaches π radians, at which point the subsequently emitted harmonic field begins to interfere destructively. All-optical QPM using counterpropagating pulses works by arranging for the overlap region of the colliding pulses to suppress emission from one or more coherence zones that would otherwise cause destructive interference. A sequence of counterpropagating pulses can allow significant enhancement of the HHG signal if constructed appropriately. Each pulse must have the correct width for suppressing the out-of-phase harmonic emission from one coherent zone, while the sequence of pulses must have the correct spacing for suppressing consecutive out-of-phase coherence zones, while allowing in-phase zones to coherently add.

The optimal shape of the counterpropagating pulses for QPM is that which most effectively suppresses destructive interference from out-of-phase zones. The overlap region between the counterpropagating and driving laser pulses corresponds to half the width of the longer counterpropagating pulse, since the pulses move in opposite directions. In other words, although the counterpropagating pulse may be, for example, 2 ps in duration, with a physical extent of ~600 μm, its overlap region with the forward propagating pulse will be only ~300 μm. We refer to this resulting overlap region as the "effective" width of the counterpropagating pulse. Thus, the optimal counterpropagating pulses will have a square temporal profile with effective width equal to a single coherence length. For a $Sech^2$ pulse, we found theoretically [59] and experimentally [27] that the optimal effective width (FWHM) of the counterpropagating pulse is $0.46L_c$.

3. In-situ measurement of the coherence of HHG in hollow waveguides

Effective implementation of QPM over many coherence zones requires a precise knowledge of the local coherence length of the HHG process within the interaction region. Coherent buildup of the harmonic signal must be suppressed efficiently only within a single zone, allowing emission from adjacent in-phase regions to add coherently (see Fig. 1). Unlike in the case of low-order nonlinear optical processes, the coherence length of the harmonic generation process cannot be easily estimated, because the local laser intensity in the medium is not known. One-dimensional models of intense laser pulse propoagation fail to match experimental data due to the dynamic ionization process and spatio-temporal reshaping of the intense laser pulse [67]. Effects that require complex 3-dimensional modeling to obtain a complete description of the process include plasma-induced defocusing, nonlinear phase modulation and focusing, energy loss due to ionization, and interference between coupled modes in a hollow waveguide. Furthermore, these effects will be quite sensitive to experimental conditions, and will have a strong influence on the local phase mismatch. Given these limitations, a direct experimental measurement of the local coherent buildup of high harmonic signal along the length of propagation of the pulse is exceedingly important. Past experiments made some progress in this respect, for example by observing Maker fringes [68, 69] as the length of the harmonic generation medium was varied. In this experiment, the phase mismatch resulted from the Guoy phase shift of a converging beam in a free-space geometry. Unfortunately, this measurement necessarily requires an alteration of the interaction medium, which can have unwanted effects on the result of the measurement.

#92162 - $15.00 USD Received 28 Jan 2008; revised 15 Apr 2008; accepted 19 Apr 2008; published 24 Apr 2008

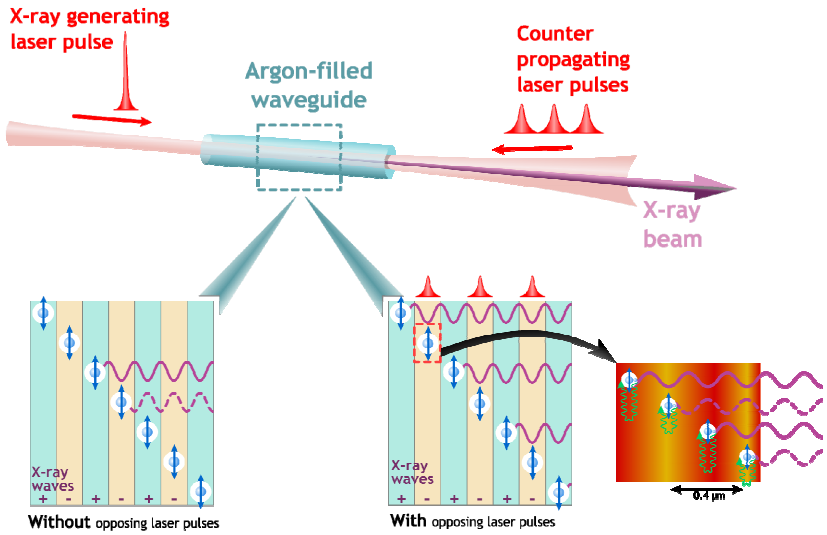

Fig. 1. Schematic for HHG in a hollow waveguide, illustrating the use of counterpropagating light to compensate for phase mismatch using all-optical quasi phase matching [1].

In recent experiments [57], we demonstrated the ability to measure, in-situ, the local coherence length of multiple harmonic orders simultaneously in a hollow waveguide. This measurement can be made over an extended propagation length, mapping how the coherence length evolves with propagation distance in the waveguide. This experiment yields previously unknown information about the evolution of the phase of harmonic light, as well as the evolution of the intensity and phase of the driving laser light.

To accomplish this measurement, the harmonic field buildup is suppressed in the overlap region of the driving laser using a single counterpropagating pulse, whose duration approximately matches the local coherence length. The harmonic signal is then monitored while this overlap region is scanned through the waveguide from exit to entrance. The experimental setup for producing the counterpropagating pulses and introducing them into a hollow waveguide is shown in Fig. 2. The output beam of a 1 kHz, Ti:sapphire CPA system is split into two parts before compression. Part of the laser energy is compressed using a grating pair compressor to a pulse duration of ~25-30 fs FWHM. This pulse, which drives the HHG process, is focused into a 150 μm inner diameter fused silica waveguide. A dilute noble gas is introduced into the waveguide through a small laser-drilled hole 5 mm from the exit, creating a slow ramp-up in pressure throughout most of the interaction region and a rapid pressure drop at the exit. The remaining laser pulse energy is partially compressed to a pulse duration of ~0.5-2 ps FWHM using a separate grating pair compressor. (The inset detail of compressor 2 shows how two counterpropagating pulses may be created, as will be discussed in Section 4.) This pulse propagates through a motorized delay stage, and is then coupled into the opposite end of the waveguide via a mirror with a 3 mm diameter hole drilled in the center. This mirror allows the forward propagating high harmonic beam to pass through, while directing a majority of the counterpropagating pulse energy into the waveguide. The fundamental light is blocked using two or more thin metal filters, chosen to transmit the photon energy band of interest. The HHG spectrum is detected using a flat-field, imaging x-ray spectrometer (Hettrick Scientific) and an x-ray sensitive CCD camera (Andor Technology).

#92162 - $15.00 USD Received 28 Jan 2008; revised 15 Apr 2008; accepted 19 Apr 2008; published 24 Apr 2008

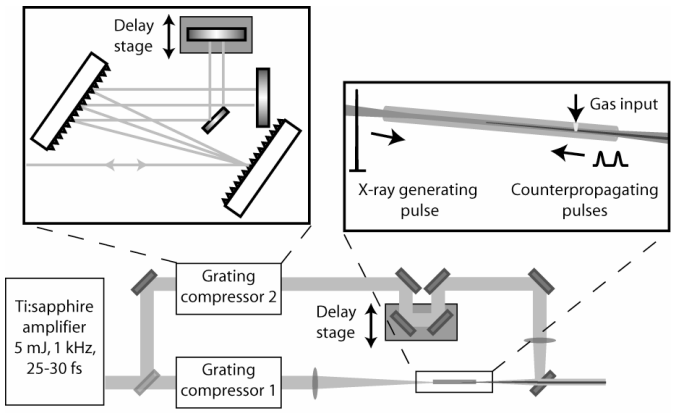

Fig. 2. Experimental setup for measuring the in-situ coherence length and implementing all-optical QPM using counterpropagating pulses.

When the overlap region is approximately the same width as the coherence length for the generation of a particular harmonic order, the counterpropagating light can have a significant effect on the overall output harmonic intensity. Because in a non phase matched regime, the overall output signal observed for any given harmonic emerges from the last coherence zone, suppression of harmonic emission from a single coherence zone anywhere in the medium will have a large effect on the overall output. Consider a simplified picture of the nonlinear conversion process in which the phase slip (coherence length) and harmonic emission strength are constant with propagation distance (see Fig. 3(a)). Emission from the final, N^{th} coherence length will be detected, while the zones preceding it will have alternating overall phase values that cancel the signal from those zones. If the harmonic field in zone N-1 is suppressed, then it will no longer destructively interfere with emission from zone N-2. In this case, the overall detected harmonic field strength will double, while the intensity increases by 4x. We refer to this as suppression from an "out-of-phase" coherence zone. Conversely, suppression of harmonic buildup from an "in-phase" coherence zone will lead to an overall decrease in the detected harmonic signal.

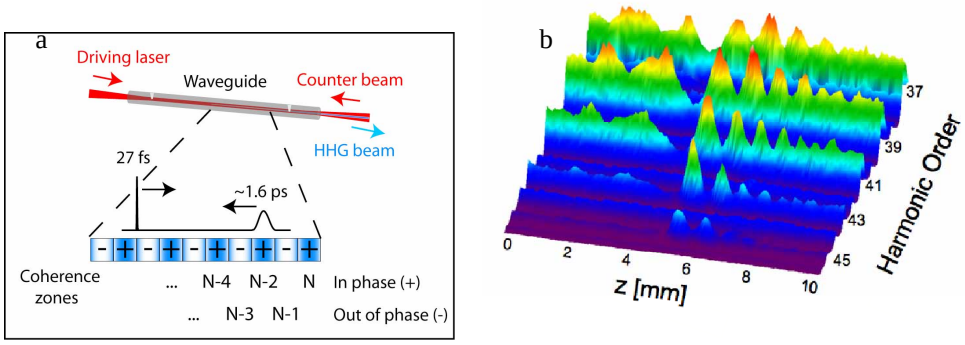

Fig. 3. Measuring the coherence length of HHG generated in a hollow waveguide. a) A schematic of the coherence zones present within a waveguide when the phase mismatch is nonzero. For N total coherence zones, the total harmonic signal detected is from only the final Nth zone, since all other "in-phase" zones can be paired with a destructively interfering "out-of-phase" zone. (b) The effect of a single counterpropagating pulse on the high harmonic emission q = 37-45 [58]. By monitoring the harmonic spectra from low pressure argon as a function of the position, z, of the overlap region between the forward- and counterpropagating pulses, the in-situ, local, coherence length can be directly visualized.

#92162 - $15.00 USD Received 28 Jan 2008; revised 15 Apr 2008; accepted 19 Apr 2008; published 24 Apr 2008

As can be seen in Fig. 3(b), distinct modulations are observed in the intensity of each harmonic order, as the overlap region that suppresses harmonic buildup is scanned through the interaction region. This harmonic light was generated in a 3.5 cm long waveguide filled with 5 torr argon. The driving pulse had a pulse energy and duration of 0.52 mJ and 25 fs, respectively, while the single counterpropagating pulse had an energy and duration of 0.2 mJ and 1.6 ps, respectively. The periodicity of these modulations is twice the coherence length, $2L_c$, allowing the local coherence length of the process to be directly measured from these data. The contrast of the modulations can be seen to vary with both location and harmonic order. This is due to the fact that the coherence length and harmonic emission strength vary with both position and harmonic order, shown in more detail below. The greatest contrast will occur when the overlap region precisely matches that of the coherence length, and when the signal strength of the two interfering zones is the same. When the counterpropagating light permits transmission from a coherence zone which has a smaller field strength than the final zone, either due to absorption by the gas medium, or a weaker harmonic emission, the contrast of the fringes will decrease. In these cases, however, weak contrast of the modulations is not an indication of poor relative coherence.

Strong contrast in the interference fringes over an extended interaction distance is then not a necessary, but a sufficient indication of strong relative coherence between harmonic emission from different locations in the waveguide. The longer the distance over which the harmonic emission maintains a good relative coherence, the more potential exists for enhancing HHG using QPM. Strong contrast in the modulations have been observed for distances over 1 cm in hollow waveguides. This shows that the waveguide geometry provides the long-range coherence necessary for implementing all-optical QPM. Ultimately, the absorption depth of the gas medium for the photon energy of interest is what limits the obtainable flux [70]. For certain photon energies, such as the "water window" region at ~2-4nm, helium has a very long absorption depth (~10's of cm) - much longer than the typical coherence length there (~10's of μm). In this region, all-optical QPM in a hollow waveguide is an ideal solution for implementing bright coherent short wavelength sources.

While the hollow waveguide geometry provides a long interaction distance by maintaining a high intensity by guiding the driving laser, the HHG process is sensitive even to small variations in the peak intensity and pulse shape of the driving field. Probing with a single counterpropagating pulse can provide information about the variation of the intensity of the driving laser. As indicated above, the energy of the driving laser pulse will vary with propagation distance due to various mechanisms such as imperfect guiding of the hollow waveguide, energy lost to the ionization process, defocusing of the light by the plasma, modebeating, phase modulation and self-focusing, and spatio-temporal nonlinear coupling. The effect of an overall decreasing laser intensity on the coherence length is to vary the level of ionization. Free electrons are strongly dispersive - even a slight change in their density will change the phase mismatch. As the laser intensity decreases, the ionization level also decreases, thereby reducing the phase mismatch and increasing the coherence length near the exit of the waveguide. This effect is shown in Fig. 4(a), where the overlap region is scanned through the waveguide. It is clear that the periodicity of the modulations increases toward the exit, indicating a lower density of free electrons, and hence a lower intensity.

Another source of variation in the driving laser intensity is the interference of propagating modes of the waveguide and spatio-temporal coupling, leading to a periodic variation of the driving laser intensity. For example, when there is a significant amount of energy propagating in both of the two lowest-order modes, EH_{11} and EH_{12}, of the 150 μm diameter waveguide, the mode beating corresponds to an on-axis intensity modulation of period ~2.2 cm. For a strong enough modulation of the laser intensity, the harmonic generation will be limited to the regions of highest on-axis intensity. This effect is shown in Fig. 4(b) which shows the detected intensity of harmonics 25 and 39, generated in argon, as the overlap region of the forward and counterpropagating pulses is scanned over the full length of a 6 cm waveguide. The counterpropagating scan reveals the presence of strong harmonic emission only in

#92162 - $15.00 USD Received 28 Jan 2008; revised 15 Apr 2008; accepted 19 Apr 2008; published 24 Apr 2008

specific regions of the waveguide. The periodicity shown in these data agrees well with that observed in a simulation of the modebeating effect (see Fig. 7(b)).

Another aspect worth noting about the data in Fig. 4(b) is where the different harmonic orders are generated within the waveguide. At z ≈ 5 cm, there is detectable emission from the 25th, but not the 39th harmonic order. This can be explained by energy loss in the driving laser field, that reduces the intensity below cutoff for the higher harmonic orders. Moreover, the absorption depth of the 25th harmonic is ~0.5 cm at the pressure used in these experiments, while the absorption depth of the 39th harmonic is ~4 cm. This explains why there is no detectable response to the counterpropagating light near the entrance of the waveguide, at z ≈ 0.8 cm.

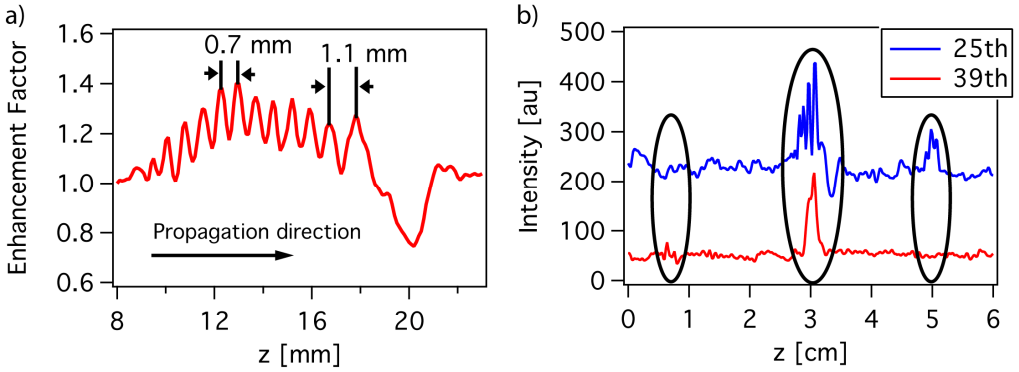

Fig. 4. Spatial variations in the local coherence length of HHG with propagation distance in a hollow waveguide. (a). Loss mechanisms lead to an increasing coherence length with propagation distance. (b). Modebeating causes the harmonic emission to be localized in the waveguide at a periodicity of ~2.2 cm.

A single counterpropagating probe pulse can also been used to gain information about the temporal dynamics of HHG. Under constant experimental conditions (i.e., gas pressure, laser intensity, ionization fraction, waveguide diameter, etc.), the coherence length should vary inversely with the harmonic order, due to the frequency dependence of the dispersion. This inverse relationship can be seen in the calculated curves of Fig. 5(a), which are based on Eq. (2).

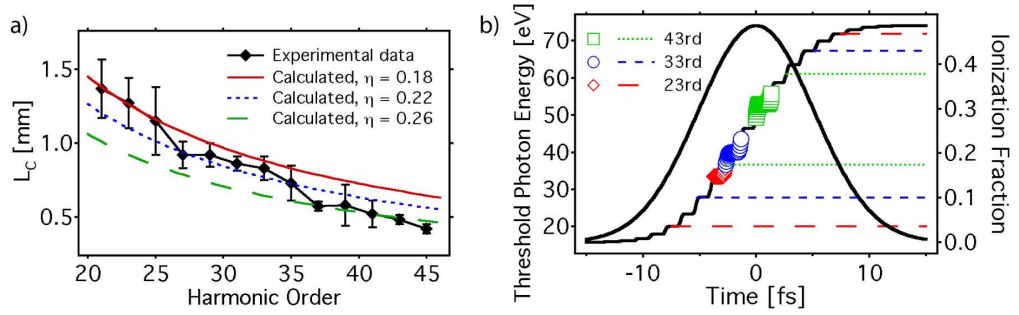

Fig. 5. (a). Coherence length vs harmonic order in 5 torr argon at a single location in the hollow waveguide, as well as calculated dependences at different levels of ionization. Measured L_C decreases faster than 1/q due to increasing ionization levels with harmonic order. (b). Time of harmonic generation within the generating ultrafast pulse for three harmonic orders, based on the measured coherence length, and the inferred ionization level calcuated using ADK ionization rates. Dotted lines indicate the energetically allowed ranges for the same harmonics, based on the cutoff rule [57].

#92162 - $15.00 USD Received 28 Jan 2008; revised 15 Apr 2008; accepted 19 Apr 2008; published 24 Apr 2008

For the data in Fig. 5(a), the coherence length for several harmonic orders generated in argon was measured at the same location, near the exit of the waveguide. When compared to the calculated curves, however, it can be seen that higher harmonic orders are generated at increasing levels of ionization. Thus, such a measurement of coherence length can be used to infer the ionization level at which each harmonic order was generated in this region of the waveguide (using Eq. 2). Knowledge of the ionization level then allows us to determine at what time within the laser pulse a particular harmonic order was generated. Figure 5(b) shows the result of such a calculation, using the Ammosov-Delone-Krainov (ADK) tunneling ionization rates [71], for three of the harmonic orders: q = 23, 33, and 43. The different levels of ionization indicate that the brightest signal for each harmonic is not generated simultaneously. Instead, the lower photon energies are generated earlier in the pulse, at a lower ionization level, than the higher photon energies. This leads to a stronger variation in the coherence length with harmonic order, since the higher order harmonics are generated in a more highly ionized, and hence more dispersive, medium.

Another temporal phenomenon is indicated by the data in Fig. 5(b). A given energy harmonic may only be generated within a limited time range of the pulse, during which the intensity is high enough, according to the cutoff rule [21]. Thus, in theory the lower harmonic orders can be generated over a longer time within the than higher harmonic orders. The horizontal dashed lines in Fig. 5(b) indicate this range for each of the three harmonics. The data in Fig. 5(b) however indicate that under our experimental conditions, the brightest harmonics, which contribute most strongly to the detected signal, are generated, not at the peak of the pulse, or even throughout the energetically allowed region, but rather when the driving laser reaches the intensity threshold to generate that harmonic.

4. Probing the coherence of HHG using two counterpropagating pulses

Spatio-temporal self focusing and plasma-induced defocusing effects can lead to laser intensity variations as the pulse propagates, regardless of the exact HHG geometry used [67, 72]. In hollow waveguide geometries, an additional effect also contributes to the laser intensity variation with propagation, since the excited propagation modes depend sensitively on the coupling conditions [73]. This situation influences harmonic generation in several ways. First, emission of the highest harmonics may be confined longitudinally to regions corresponding to maximum laser intensity, as shown in Fig. 4. Second, since the ionization rate of the gas medium is proportional to the intensity, there will be a large variation in the single-atom efficiency for harmonic generation along the waveguide. This variation in the efficiency significantly influences the harmonic signal detected at the exit of the waveguide.

A scan of the collision region of the driving laser pulse and a single counterpropagating pulse through several coherence zones can result in coherent oscillations in the detected HHG signal, such as those shown in Fig. 3(b). In this case, the length and harmonic emission efficiency of the zones are approximately constant with propagation distance. As discussed above, the size of the coherence lengths as well as their dynamics in space and time, can be obtained from these oscillations. This information is essential for understanding how harmonics are generated and how the phase mismatch may be compensated. However, when the harmonic emission varies significantly along the propagation direction (e.g. due to mode beating and nonlinear laser-plasma interactions), a scan of a single counterpropagating pulse will not give rise to clear oscillations in the HHG signal. Instead, regions of large enhancement in the HHG signal are typically observed. Thus, it is necessary to develop a new technique for probing the coherent buildup of harmonics under these conditions.

In this section, we show that it is possible to probe the coherence and measure the coherence length for HHG, even in the presence of laser intensity variations. This is done using a pair of counterpropagating pulses. When the scan of a single counterpropagating pulse does not show coherent ringing, we can measure the relative phase between harmonic emission from different locations in the waveguide using two counterpropagating pulses whose separation is continuously varied. For this measurement, the collision region of one of the counterpropagating pulses is fixed in space, while the second counterpropagating pulse is

#92162 - $15.00 USD Received 28 Jan 2008; revised 15 Apr 2008; accepted 19 Apr 2008; published 24 Apr 2008

scanned through the region of interest, to determine the mutual phase of the HHG emission from different regions in the medium.

We first theoretically describe HHG emission under the influence of counterpropagating pulses. The harmonic field at the output of the nonlinear medium, of length L, can be simply expressed as -

$$E_{HHG}(L) = \int_0^L E^0_{HHG}(z) \exp\left(i \frac{\pi}{L_C(z)} z \right) dz, \quad (6)$$

where $E^o_{HHG}(z)$ is the strength of generated harmonic field as a function of the propagation distance, z, and $L_C(z)$ is the z-dependent coherence length. We now consider two representative regimes, which model the two experimental observations described above.

Regime 1: $E^0_{HHG}(z) \sim E^0_{HHG}$ and $L_C(z) \sim L_C$

This regime is characterized by ringing in the detected HHG signal when the collision region of a single counterpropagating pulse and the driving laser pulse is scanned through the interaction region (as seen in Fig. 3(b)). In this regime, the strength of the harmonic emission and the coherence length are approximately constant with propagation distance. Except for the final, N^{th}, coherence zone, all the preceding zones are paired with an identical zone of opposite overall phase that destructively interferes (se Fig 3(a)). Without a counterpropagating pulse, the only emission detected is that from the N^{th} zone. When a counterpropagating pulse suppresses the emission from one of those preceding zones, the emission from its "partner" zone will interfere with the N^{th} zone. If all zones are constant in length and emission strength, the suppression of any zone will either double the total field exiting the waveguide, or completely suppress it. Thus, as the collision region is scanned through the nonlinear medium, high contrast fringes appear in the detected HHG signal.

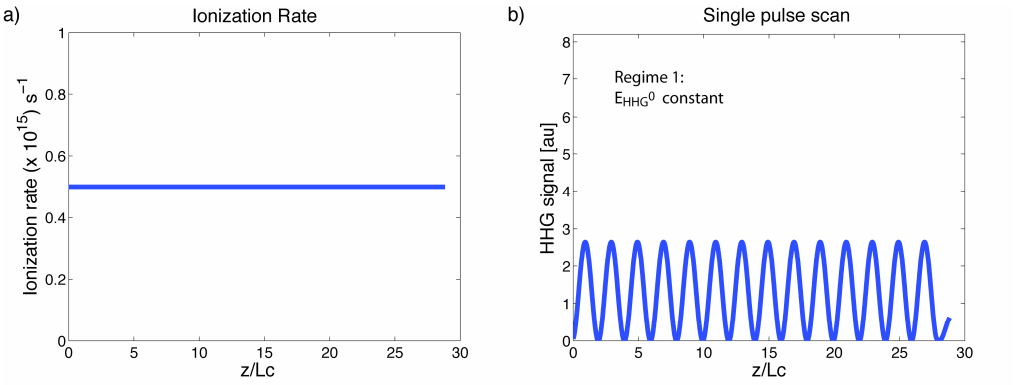

Fig. 6. Simulation of a scan of counterpropagating pulse when the strength of harmonic field and L_c do not vary along propagation. a) A constant ionization rate with propagation and b) the variation in the intensity of the detected harmonic signal for the scan of a single counterpropagating pulse, showing coherent ringing.

A simple calculation of this effect is shown in Fig. 6. For this calculation, $E^0_{HHG}(z)$ is assumed to be constant with propagation distance and proportional to the ionization rate, which was calculated for typical experimental parameters for HHG in argon gas. Figure 6(a) shows the constant ionization rate profile as a function of propagation distance. The simulation of the counterpropagating pulse scan is performed using Eq. (6) as a function of the position of the overlap region of the pulses, in which the harmonic signal is completely suppressed. The counterpropagating pulse is approximated to be square in temporal profile, with an effective width equal to the coherence length, and with the optimal laser intensity

#92162 - $15.00 USD Received 28 Jan 2008; revised 15 Apr 2008; accepted 19 Apr 2008; published 24 Apr 2008

needed to suppress HHG emission completely [58, 59]. Figure 6(b) shows the coherent ringing in the harmonic output that is predicted in this regime.

Regime 2: $E^0_{HHG}(z)$ and/or $L_C(z)$ changes significantly with propagation distance.

This regime is characterized by a significant change of the detected HHG signal when the collision region of a single counterpropagating pulse and the driving laser pulse is scanned through the interaction region. A significant variation in $E^0_{HHG}(z)$ and/or $L_C(z)$ means that the emitted high harmonic signal is varying significantly along its propagation. As an example, we consider the case where L_C is constant, and the harmonic emission strength oscillates with propagation distance (Fig 7(a)). Now the final coherence zone is weak relative to the preceding zones. If the collision point suppresses harmonic emission from a zone which has a much stronger emission, then its "partner" zone will dominate the spectrum, having only a small modulation due to interference from the much weaker N^{th} zone. Figure 7 shows the results of the propagation simulation for this case. Figure 7(a) shows the profile of the ionization rate as a function of distance in the medium for changing laser intensity. This profile was generated taking into account the interaction of the two lowest order coupled modes in a hollow waveguide with inner diameter 150 μm. For this calculation, the energy of the driving laser beam was divided between the two modes, with 67% of the laser energy in the EH_{11} mode and 33% of the energy in the EH_{12} mode. The intensity profile as a function of both propagation distance and waveguide radius is shown in Fig. 7(c). The 1D ionization rate was calculated from the intensity variation at the central axis of the waveguide. For the simulation of a single pulse scan, the same calculation was performed as for Fig. 6(b), but now with a longitudinally-varying ionization rate. The coherent ringing disappears, and the HHG can be enhanced greatly with a single counterpropagating pulse (Fig. 7(b)).

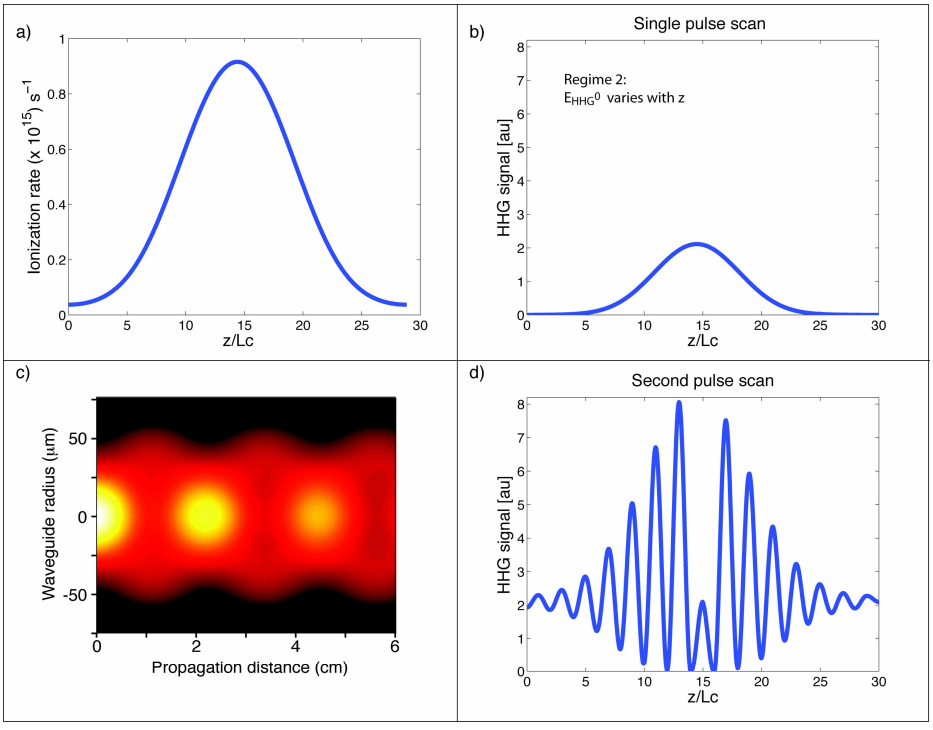

Fig. 7. Simulation of the HHG output when a) the ionization rate varies due to mode beating, for b) the scan of a single counterpropagating pulse, and d) the scan of a second counterpropagating pulse when the first is held fixed at z/L_c=15. The model assumes an interaction between the two lowest order coupled modes, which induce a periodic variation of intensity, shown in c).

#92162 - $15.00 USD Received 28 Jan 2008; revised 15 Apr 2008; accepted 19 Apr 2008; published 24 Apr 2008

In order to directly observe the coherent buildup oscillations in such a regime with significant longitudinal variations, a two-pulse counterpropagating probe is required. For these experiments, the first counterpropagating pulse is held at a fixed position where the enhancement is large, while the second counterpropagating pulse is scanned through the nonlinear medium. This second scan probes the relative coherence between the bright emission now detected due to the presence of the first pulse, and the HHG emission throughout the rest of the region. In this case, the harmonic emission from different zones is of similar strength, resulting in strong contrast fringes. A simulation of this effect is shown in Fig. 7(d), where the first pulse is held fixed near $z/L_c = 15$. When the two pulses are exactly overlapped, the signal remains as though only one pulse was present. However, when the pulses are separated by a distance $2L_C$, the signal further increases by about a factor of four, which is the increase in intensity expected when the harmonic field is doubled. The ability to continuously change the distance between the two counterpropagating pulses pinpoints the exact separation of the pulses required for the greatest enhancement of the HHG signal. Additionally, the periodicity of the fringes provides a measurement of the local coherence length in this second regime, which was previously inaccessible.

Experimentally, both of the above regimes have been observed by scanning a single counterpropagating pulse through the medium. Figure 8(a) shows a typical data set obtained by scanning a single counterpropagating pulse through a region of strong intensity variation. For these data, the interaction region consists of 8 torr of argon in a 6 cm long waveguide. The HHG generation pulse had a duration and energy of 27 fs and 0.47 mJ, respectively, while the counterpropagating pulse had a duration and energy of ~1 ps and 0.08 mJ, respectively. The effect of the single counterpropagating pulse is to strongly enhance the harmonic flux over a distance of 4 mm or more. However, no coherent ringing is observed by scanning a single counterpropagating pulse.

This situation changes dramatically when a pair of counterpropagating pulses are used. In order to create a pair of pulses with adjustable separation, a mirror in compressor 2 directs half the frequency-dispersed light to a separate retroreflector (see Fig. 2). This retroreflector is mounted on a delay stage, to control the timing of one half the spectral energy in the beam relative to the other. Linear chirp is added by the compressor so that each pulse is approximately 1 ps in duration. Thus both the width and the separation of the two counterpropagating pulses are independently and continuously controllable variables.

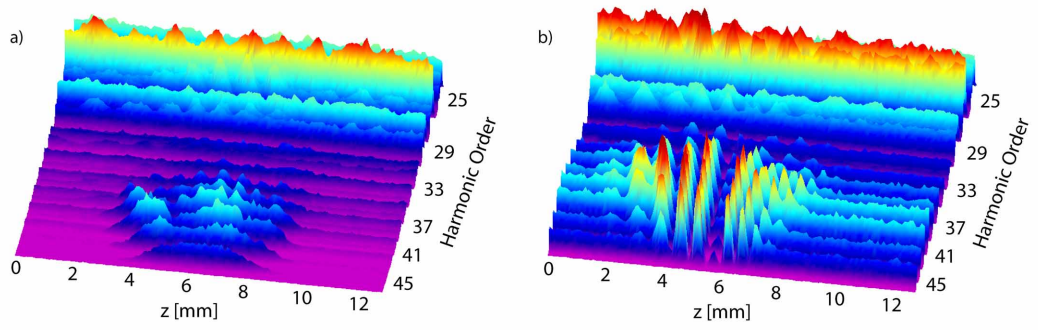

Fig. 8. Harmonic spectra observed in 8 torr argon as a function of the position of the overlap region, z, between the forward- and counterpropagating pulses. a) A single counterpropagating pulse is scanned through the interaction region, showing little coherent ringing. b) A second counterpropagating pulse is scanned through the interaction region, while the first remains stationary at $z \approx 6$ mm. Here, strong coherence is observed.

The result of scanning a second counterpropagating pulse, while holding the first fixed in position, is plotted in Fig. 8(b). This plot reveals the relative coherence of the harmonic emission in this region. The first counterpropagating pulse is held stationary at position $z \approx$

#92162 - $15.00 USD Received 28 Jan 2008; revised 15 Apr 2008; accepted 19 Apr 2008; published 24 Apr 2008

6 mm, while the second pulse is scanned through the same region. Modulations appear with strong visibility, demonstrating the strong relative coherence of the two regions while also providing a measurement of the coherence length. The signal is weak at the position where the two counterpropagating pulses are exactly overlapped, since they suppress coherent addition in the same region of emission. However, when the pulses are separated by $2L_C$, the signal is enhanced dramatically, because two coherence zones from a region of strong emission are permitted to add coherently. Further enhancement could be achieved by adding more pulses to the counterpropagating pulse train, while optimizing the width and separation of each pulse.

These measurements constitute a new technique for probing the local phase mismatch as well as the spatial and temporal emission of HHG. Simulations of the counterpropagating pulse scans (i.e., Fig. 7) show clear qualitative agreement with the observed data, providing evidence for the validity of the simple model presented. Because the largest enhancements due to all-optical QPM have been observed in this second regime, where the harmonic emission varies strongly with propagation distance, this approach yields the necessary information required to design optimal pulse trains for all-optical QPM.

One future application of this two-pulse probing technique is to probe the relative coherence of HHG at greater separations (>1 cm) within the hollow waveguide. Because HHG is most strongly generated in regions of strong laser intensity on-axis, nonlinear reshaping and modebeating can limit strong emission to a several millimeter long region separated by cm-scale distances. For a 6 cm length, 150 μm hollow waveguide, there are ≈ 3 regions of high laser intensity. The coherent addition of light from each of these three intense regions could lead to significant further enhancements of HHG.

5. All-optical quasi-phase matching using counterpropagating pulse trains

Once the coherence lengths for different harmonic orders are known, a train of counterpropagating pulses with the correct width and separation can be used to suppress emission from multiple, out-of-phase coherence zones. This enables buildup of the x-ray signal from in-phase zones only, leading to enhancement of the HHG signal [27, 58-60]. The first experiment to probe harmonic generation in the presence of a counterpropagating pulse was performed by the Peatross group using harmonics generated in gas jets [74] and gas cells [75]. Under well phase-matched conditions, they observed suppression of the harmonic signal from argon and neon, but not in helium. When the phase mismatch was deliberately increased by changing the focusing conditions, enhancement was observed, but not above what could be achieved by geometrical optimization of the phase matching conditions. Hence, while an enhancement of the harmonic signal was observed due to the presence of counterpropagating light, this enhancement was not an improvement above other phase matching techniques. Moreover, they were unable to match the width of the counterpropagating pulse to the coherence length without the ability to measure the coherence length. The potential enhancement through QPM was also ultimately quite limited, due to the fact that the length of the interaction region was of the order of the coherence length, in some cases due to the width of the gas jet, while in others due to the absorption depth of the gas used.

We recently demonstrated substantial QPM enhancement of HHG above what can be obtained simply by optimizing phase matching conditions. In this work, we examine regimes where harmonic generation cannot be truly phase matched because of the high level of ionization in the medium; i.e. $\eta >> \eta_c$. By using a sequence of three counterpropagating pulses, we demonstrated an enhancement factor of ~300 at photon energies near 70 eV for harmonics generated in argon. This enhancement due to all-optical QPM elevates the HHG signal from argon at 70 eV to a level comparable to that from conventionally phase matched helium at this energy. We also demonstrated an enhancement of more than 100x at photon energies near 140 eV in helium, using only two counterpropagating pulses. At this photon energy, HHG cannot be conventionally phase matched in any gas for the driving laser wavelength used. These results show the potential of all-optical QPM for further substantial enhancements of HHG when additional counterpropagating pulses are employed. This technique is shown to be applicable to HHG even in the presence of high levels of ionization

#92162 - $15.00 USD Received 28 Jan 2008; revised 15 Apr 2008; accepted 19 Apr 2008; published 24 Apr 2008

and dynamically changing phase mismatch, and easily scalable to longer pulse trains for larger enhancements. All-optical QPM is particularly promising for enhancing emission at high photon energies, which are severely limited in flux by a large phase mismatch.

For enhancing harmonics near 70 eV in argon, the gas was introduced at a pressure of 10 torr into an 11 cm long waveguide. The collision point of the forward and counterpropagating pulses was scanned over a 2 cm region centered approximately 4 cm from the entrance. In this experiment, the separation of the counterpropagating pulses was set using a static phase mask: the frequency-dispersed beam in the second compressor was divided into three segments of approximately the same energy, each traveling through a different thickness of glass to adjust its separation. The HHG spectra detected in the presence of zero, one, and three counterpropagating pulses are shown in Fig. 9(a).

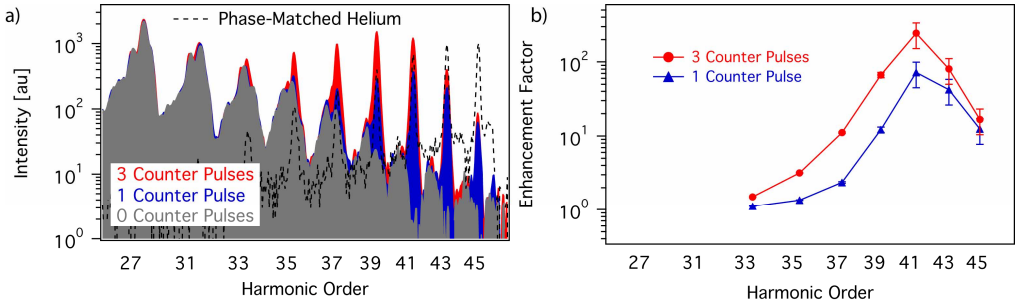

Fig. 9. (a). Observed harmonic emission from argon for no (gray), one (blue), and three (red) counterpropagating pulses. Phase-matched emission from 100 torr helium (dashed black) is included for comparison. (b). Enhancement factor as a function of harmonic order, for one (blue) and three (red) counterpropagating pulses [58].

In this experiment, the harmonic emission varies significantly along the propagation direction, corresponding to the second regime described in Section 4. In this regime, a single counterpropagating pulse can significantly enhance the total output of the HHG signal, although coherent ringing is not observed. Indeed, in our experiment, any one of the three counterpropagating pulses enhances the 41st harmonic order by approximately two orders of magnitude (Fig. 9(b)). The first pulse intersects with the driving laser pulse within the region where the harmonic emission is most efficient. As a result, bright harmonic generation from that region is now detected at the output of the waveguide. The second and third pulses enhance the signal further, but by a much smaller factor, corresponding to the addition of similar strength coherence zones. The enhancement in this case is likely limited by imperfect delay between the counterpropagating pulses, since the pulse train is created using a static, nonadjustable, phase mask.

The emission of helium, under similar experimental conditions, but at the phase matching pressure of 100 torr, is also plotted in Fig. 9(a) as a comparison of the brightness of harmonic emission at this energy. The brightness of the harmonics up to the 43rd order are comparable or brighter than those from helium. Although the emission from helium may in principle be phase matched, the absorption depth is much smaller at the phase matching pressure (~3 mm vs. ~3 cm in 10 torr Ar). Hence all-optical QPM is able to surpass the brightness of conventional phase matching in a waveguide, even with only three counterpropagating pulses. The QPM enhanced flux is estimated to be ~10^{10} photons/s per harmonic near the 41st harmonic order. Moreover, further enhancements can still be obtained in argon by the addition of more counterpropagating pulses, since the absorption depth is still much longer than the region over which the HHG emission was summed, ~3 mm.

The addition of the second and third counterpropagating pulses leads to other distinct effects. The enhancement is selective, enhancing the 41st harmonic order more strongly than the adjacent orders. Because the coherence length of the harmonics varies by at least 1/q, as

#92162 - $15.00 USD Received 28 Jan 2008; revised 15 Apr 2008; accepted 19 Apr 2008; published 24 Apr 2008

described in Section 3, a pulse train with a given delay between the individual pulses will selectively enhance a single harmonic order. The addition of more counterpropagating pulses will not only enhance the HHG signal further, but will become more selective of a single harmonic order. Subsequent work, using four counterpropagating pulses (Fig. 10), shows a larger enhancement factor of ~600, along with this strong selectivity, of the 41st harmonic order. This feature of all-optical QPM is particularly attractive for applications of HHG that require a narrow spectral bandwidth – for example, molecular and surface spectroscopy or imaging.

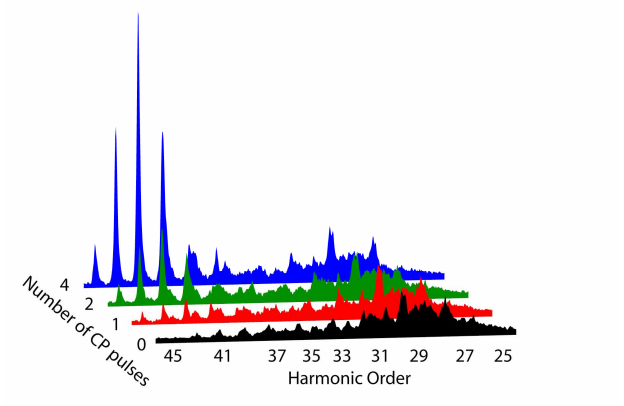

Fig. 10. All-optical QPM of HHG in argon, with a train of up to four counterpropagating pulses.

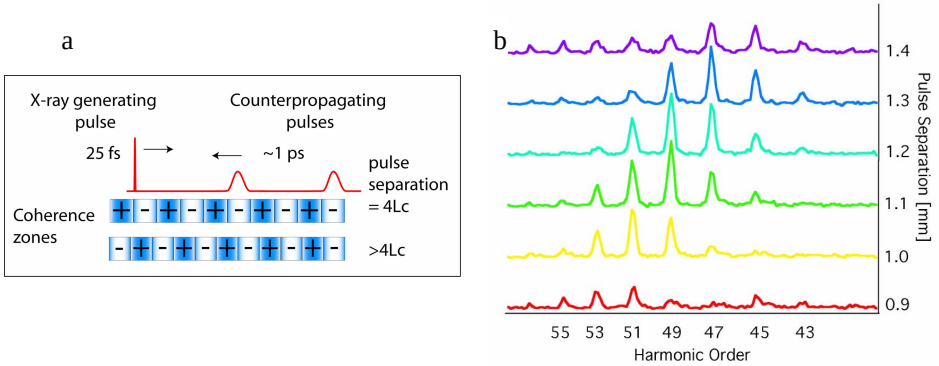

Fig. 11. Tuning the selectivity of all-optical QPM using two counterpropagating pulses, by varying their separation. The effective pulse widths of each pulse was ~300 μm. A schematic illustrating this effect is shown in a).Enhancement occurs when the pulse separation is $2^N L_C$. Selectivity improves when N >1. HHG spectra from argon, in b), show the shift of the enhancement with harmonic order as the separation between the pulses is varied.

The selectivity of all-optical QPM can be improved further if the counterpropagating pulses suppress out-of-phase coherence zones that are not adjacent, but are farther apart. Figure 11(a) illustrates this effect: the size of the coherence zones for two different harmonic orders will be slightly different due to the frequency dependence of the dispersion. A given pair of counterpropagating pulses can be adjusted to match the spacing of out-of-phase coherence zones for one harmonic order, but will not match the spacing of another harmonic order. This effect becomes more prominent the greater the separation between the pulses. This can be shown by varying the separation of two counterpropagating pulses. Figure 11(b) shows enhanced spectra of HHG in argon, at different pulse separations. The width of each counterpropagating pulse was kept constant at ~300 μm, but the delay between them was continuously varied, around a pulse separation of approximately 4 L_C. A shift can be clearly

#92162 - $15.00 USD Received 28 Jan 2008; revised 15 Apr 2008; accepted 19 Apr 2008; published 24 Apr 2008

seen in the harmonic order that is most strongly enhanced, depending only on the separation of the pulses.

For the data shown in Fig. 12, helium gas was introduced at a pressure of 110 torr into a 6 cm waveguide. The collision point of the forward and counterpropagating pulses was scanned over a 2 cm region near the exit of the fiber. The two counterpropagating pulses used were formed by the setup of compressor 2, shown in Fig. 2, so that their width and separation were individually controllable. While the coherence regime for this system was also of the second type described in Section 4, the coherence length was measured by scanning the time delay between the two counterpropagating pulses to observe strong contrast coherent oscillations. This also allowed a careful tuning of both the width of each pulse and the separation of the pulses for the maximum enhancement. Figure 12(a) shows the spectra obtained with zero, one, and two counterpropagating pulses present. With two counterpropagating pulses, the enhancement reached factors of 150 and 120 for the 87th and 89th harmonic orders, respectively. The enhancements for harmonic orders q = 79-95 are shown in Fig. 12(b). These harmonic orders, at photon energies around 140 eV, were empirically shown to be generated at an ionization level of 1.7%, or about 3x the critical ionization level for helium: η_{cr} = 0.5%.

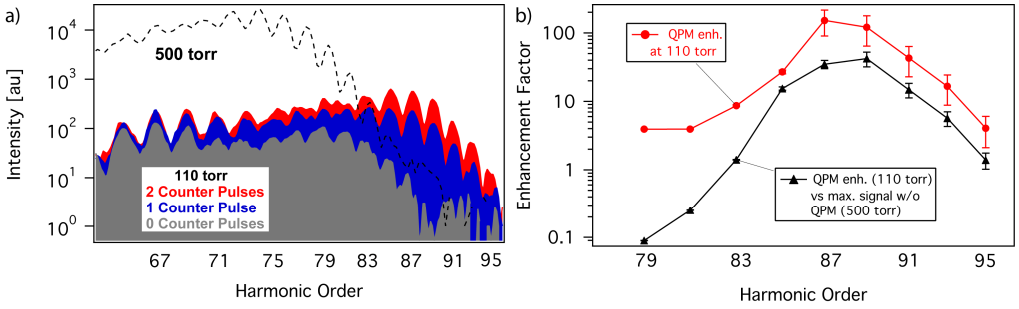

Fig. 12. (a). Observed harmonic emission from 110 torr helium for no (gray), one (blue), and two (red) counterpropagating pulses. The dotted curve shows harmonic emission under similar laser conditions, but at a pressure of 500 torr, which is optimal for conventionally phase matching lower harmonic orders, below q = 77. (b). Enhancement factors for harmonic orders q = 79-95. Red circles show the ratio of the quasi-phase matched emission obtained using a train of two counterpropagating pulses to that without counterpropagating light at a pressure of 110 torr. Black squares show the ratio of quasi-phase matched emission at 110 torr to that without counterpropagating pulses at a pressure of 500 torr [27].

Harmonic orders below q = 79 generated in helium can be phase matched by adjusting the gas pressure, since they can be generated at an ionization fraction below η_c for the laser parameters used. Therefore, as a measure of the absolute enhancement of all-optical QPM, the gas pressure was increased to optimize the brightness of the HHG emission, particularly for the highest observed harmonic orders, with no counterpropagating pulses present. The overlay in Fig. 12(a) shows the spectrum present at a optimal pressure of 500 torr, clearly showing that all-optical QPM using helium at 110 torr increases the brightness of harmonic orders q = 83-95 better than simply optimizing the pressure. At q = 89, the enhancement achieved by QPM corresponds to a flux 40x the maximum emission achieved by pressure tuning alone.

Further enhancements and stronger selectivity of high harmonic emission at even higher photon energies can be accomplished using a train of many counterpropagating pulses, allowing coherent addition of HHG over longer interaction distances. However, the most efficient implementation of all-optical QPM will require more sophisticated techniques for producing counterpropagating pulse trains. Pulse shaping is a possible technique for creating customized pulse sequences. It could be used to match the critical timing and duration parameters of the pulses to the spatially varying coherence length present in the waveguide.

#92162 - $15.00 USD Received 28 Jan 2008; revised 15 Apr 2008; accepted 19 Apr 2008; published 24 Apr 2008

Moreover, it could adjust the amplitude of each pulse in order to partially shift, by π radians, the out-of-phase coherence zones, further increasing the potential enhancement [58].

The ability to implement longer pulse trains will extend the usefulness of this technique to higher photon energies. The shorter coherence lengths inherent to the generation of higher photon energies will require more counterpropagating pulses to achieve similar enhancement factors. However, the outlook is very promising for extending all-optical QPM to higher photon energies. The demonstration of strong coherence of the HHG process over extended distances in hollow waveguides shows that in-phase emission from many coherence zones can be coherently summed. Moreover, the laser energy needed for each counterpropagating pulse decreases with increasing photon energy for two major reasons. First, the intensity of the counterpropagating pulse necessary for suppressing coherent buildup decreases linearly with harmonic order. Second, for shorter coherence lengths, the required duration of the counterpropagating pulses also decreases.

Finally, the temporal and spatial coherence of HHG-based sources may also be improved by all-optical QPM. During the electron rescattering process, there are two quantum paths corresponding to the same kinetic energy that contribute to a given harmonic in the plateau region. The so-called "long" trajectory results from ionization immediately after the peak of the laser field, for which the electron returns to the atomic core up to a full optical cycle later. For the "short" trajectories, the time in the continuum is always < ¾ of an optical cycle. Due to differential nonadiabatic blueshifting of the harmonic light [76, 77], these separate trajectories may be distinguished in the spectral data. Probing of the coherence length has shown that emission from the long and short trajectories have distinct coherence lengths, even for the same harmonic order. Thus, all-optical QPM can enhance a single harmonic corresponding to either the long or short trajectory [60]. Since spatial and temporal coherence are degraded due to interference of emission from different quantum trajectories, this approach the temporal and spatial coherence, the selectivity, and the flux of a single harmonic. These qualities will become especially important as imaging and measurements requiring strong coherence are implemented at ever smaller wavelengths.

6. Phase matching at keV photon energies using quasi-CW counterpropagating beams

Recent exciting theoretical work [48] shows that all-optical QPM in theory can be used to implement phase matching even at very high, keV, photon energies corresponding to very short coherence lengths. The all-optical QPM techniques using counterpropagating pulse trains that were discussed above are useful for harmonic orders for which the coherence lengths correspond to ten or more optical wavelengths. At the intensities required for generating keV energies, however, the coherence lengths are typically on the order of microns. In this regime, the coherence length is of the same order as the periodicity of the oscillations in the phase of the emitted harmonic that are induced by the counterpropagating field. Thus, a counterpropagating pulse train cannot be used for effective suppression of the HHG process in out-of-phase zones. Instead, a quasi-CW, counterpropagating IR beam can be used to adjust the phase of the emitted harmonic field and allow phase matching of the HHG process. This process is illustrated schematically in Fig. 13 [48].

In this shot coherence length regime, the coherent buildup of the HHG field may be described as:

$$E_{HHG}(L) \propto \int_0^L \exp\left[i\left(\frac{\pi z}{L_C} + A\cos\left(\frac{2\pi z}{\Lambda} \right) \right) \right] dz, \tag{7}$$

where L is the total length of the nonlinear medium, $\Lambda = \lambda_2/2$ is the periodicity of the intensity interference pattern, λ_2 is the wavelength of the counterpropagating IR beam, and A is the amplitude of the induced phase modulation. Interestingly, Eq. (7) describes grating-assisted phase matching in conventional (i.e., low-order) nonlinear optics [41]. In that case, the sinusoidal term in Eq. (7) results from periodic variations in the linear susceptibility. Tuning the periodicity of the phase-shift oscillation (by changing the wavelength of the

#92162 - $15.00 USD Received 28 Jan 2008; revised 15 Apr 2008; accepted 19 Apr 2008; published 24 Apr 2008

counterpropagating, quasi-CW IR beam) to twice the coherence length, $\Lambda = \lambda_2/2 = 2L_c$, and assuming that $L = m\Lambda$, where m is a positive integer, the integral in Eq. (7) simplifies to

$$E_{HHG}(L) \propto L \cdot J_1(A), \tag{8}$$

where J_1 is the first-order Bessel function of the first kind. It is now clear that the optimal value for the amplitude of the induced oscillations in the phase shift is $A \approx 1.84$, for which $J_1(A)$ is maximal. The amplitude of the oscillations is proportional to the amplitude of the counterpropagating quasi-CW beam (since the phase shift is proportional to the intensity of the harmonic driving field) and can therefore be adjusted to its optimal value.

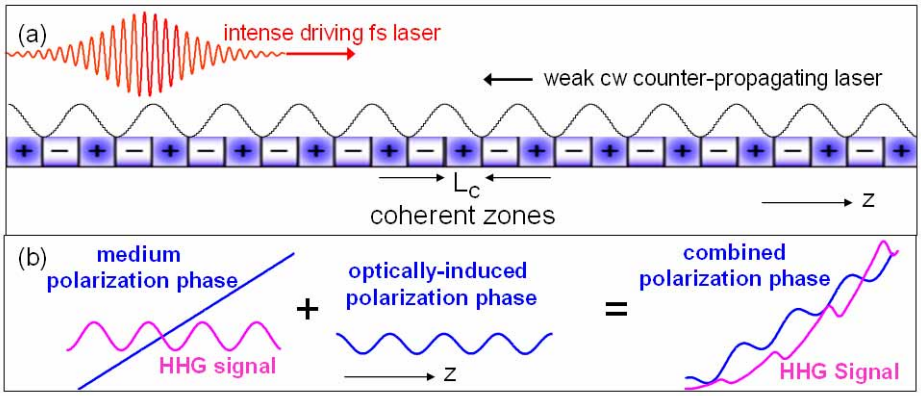

Fig. 13. (a). Schematic of optically-induced phase matching in high harmonic generation by quasi-CW counterpropagating light. (b). The combination of the medium phase mismatch and the optically induced sinusoidal oscillation in the phase of the high-order polarization results in a correction of the phase mismatch associated with the frequency conversion process. The optically induced oscillation in the phase of the high-order polarization is formally equivalent to the presence of oscillations in the refractive index for the driving laser. Variations in the refractive index were suggested for correcting the phase mismatch in low order harmonic generation via grating-assisted phase matching [48].

Next, we present a specific numerical example of grating-assisted phase matching in HHG in a pre-formed plasma waveguide [31, 78]. We consider a 20 fs driving laser pulse at λ_o = 0.8 μm, with peak intensity I_0=5.5 x 10^{13} W/cm^2, propagating in a medium that consists of doubly ionized Ne ions (ionization potential 63.45 eV) at a pressure of 70 torr. In addition, a weak (I_B = 3.5 x 10^8 W/cm^2) beam at λ_2 = 1.6 μm propagates in the reverse direction (Fig. 13). Figures 14(a) and 14(b) show that the flux of harmonic orders 647 ± 36 (corresponding to photon energies 990 ± 50 eV), for a propagation distance of L = 200 μm, is enhanced ~ 4 x 10^4 times. Moreover, this enhancement is far from saturation and therefore we expect that the signal would continue to increase over greater propagation lengths (short distances were selected to demonstrate phase matching using a reasonable computation time). The inset of Fig. 14(b) shows that $L_C \approx 0.4$ μm for harmonic order q = 647, thus matching the condition $\Lambda = 2L_c$ (the periodicity of the intensity interference grating and the phase-shift oscillations are $\Lambda = \lambda_2/2$ = 0.8 μm). The selectivity of this grating-assisted phase matching scheme is highlighted in Fig. 14(c), which plots the harmonic spectral intensity in the phase matching spectral region on a linear scale (log scale shown in Fig. 14(a). Figure 14(d) shows the intensity of the harmonics in the spectral window q = 647 ± 36. The envelope of the fields of harmonic orders 613, 649, and 681 (marked by arrows in Fig. 14(c) are plotted in the inset. The observed confinement of each harmonic to time windows of 1-2 fs results from the changing ionization level along the pulse. As the plasma density increases (corresponding to

#92162 - $15.00 USD Received 28 Jan 2008; revised 15 Apr 2008; accepted 19 Apr 2008; published 24 Apr 2008

the ionization level increasing from $\eta = 2.00$ to 2.05) the coherence lengths shorten and hence lower harmonic orders become more optimally phase matched. This observation suggests that the bandwidth of the generated harmonics can be controlled by varying both the degree and temporal dynamics of self-ionization.

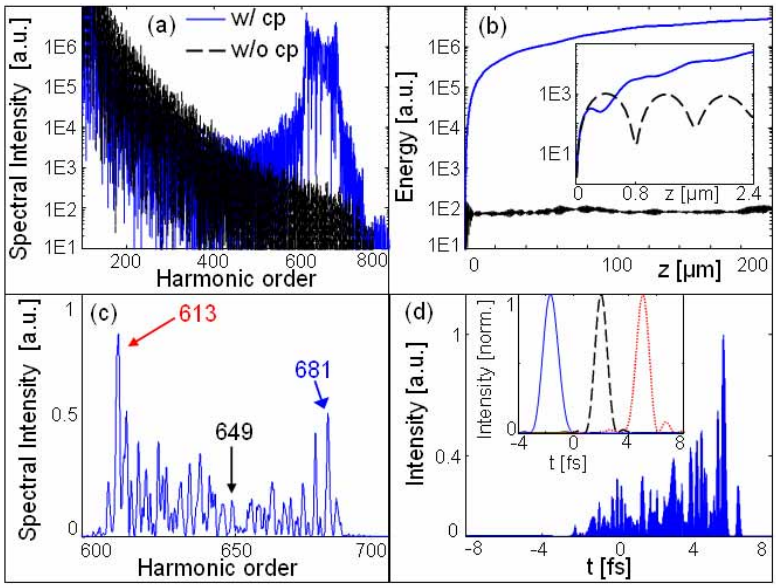

Fig. 14. Grating-assisted phase matching using counterpropagating light. (a). Harmonic spectral intensity with (solid blue) and without (dashed black) a counterpropagating field.
(b). Harmonic signal versus propagation distance in the spectral window q = 647 ± 36, with (solid) and without (dashed) a counterpropagating field. The inset shows the signal in harmonic order q = 647 in the first 2.4 mm, showing that L_C = 0.4 mm. (c). Harmonic spectral intensity in the phase matching spectral region on a linear scale. (d). Temporal profile of the intensity of harmonics q = 600-700. The inset shows the intensity in harmonics 613 (solid), 649 (dashed), and 681 (dotted) that are marked by arrows in c).

7. Conclusions and future work

The work presented here provides unprecedented access to the dynamical coherent build-up of high-order harmonic generation for the first time. The use of counterpropagating light has been demonstrated as a flexible and easily implemented technique for probing high harmonic generation both temporally and spatially, as well as the dynamics of an intense driving laser field propagating through a plasma. This works also demonstrates that the use of all-optical quasi phase matching is a powerful tool for combating the problem of dephasing of the high harmonic generation process, which is the predominant technical challenge in creating bright, coherent beams of x-rays. In particular, the flexibility of all-optical QPM allows fine tuning of the phase correction, and has been shown to be effective over a range of different photon energies and different plasma conditions. In the future, all-optical QPM using counterpropagating fields has the potential not only for producing bright beams of coherent x-rays up to photon energies > keV, but also for manipulating the spatial and temporal characteristics of the emission [60].

Acknowledgments

We gratefully acknowledge support for this work from the NSF Engineering Research Center Grant No. EEC-0310717 and the Department of Energy NNSA. A. Lytle acknowledges support from a National Science Foundation Graduate Research Fellowship.

#92162 - $15.00 USD Received 28 Jan 2008; revised 15 Apr 2008; accepted 19 Apr 2008; published 24 Apr 2008